

Received August 12, 2021, accepted August 19, 2021, date of publication August 24, 2021, date of current version August 30, 2021.

Digital Object Identifier 10.1109/ACCESS.2021.3106912

A Hybrid Regularization Operator and Its Application in Seismic Inversion

YANGTING LIU^{1,2}, CHENGUANG LIU^{1,2}, CHENGLIANG XIE³, AND QING-XIAN ZHAO³

¹First Institute of Oceanography, Ministry of Natural Resources, Qingdao 266061, China

²Qingdao National Laboratory for Marine Science and Technology, Qingdao 266237, China

³Guangzhou Marine Geological Survey, Guangzhou 510000, China

Corresponding author: Yangting Liu (yangting.lau@gmail.com)

This work was supported in part by the National Key Research and Development Program of China under Grant 2017YFC0307400, in part by the National Natural Science Foundation of China under Grant 41804131, in part by the Shandong Provincial Natural Science Foundation, China, under Grant ZR2018QD003, and in part by the Qingdao National Laboratory for Marine Science and Technology under Grant QNLM201710.

ABSTRACT Seismic inversion is an effective tool to estimate the properties of subsurface strata from seismograms. However, the intrinsic ill-posedness of the inversion problem causes the inverted subsurface properties to be easily polluted by inversion errors due to the random noise in the observed data. The inversion errors make it difficult to interpret the geological features of subsurface strata, especially their boundaries and textures. To recover high-fidelity inversion results from noisy observed data, we developed a hybrid total-variation (HTV) regularization operator in this research. Compared with the conventional total-variation (TV) regularization, the HTV regularization has two advantages when applied in seismic inversion. One advantage is that HTV regularization overcomes the typical staircase effect of conventional TV regularization while maintaining the advantage of TV regularization in edge-preserving properties. The determination of regularization parameters is also a difficult problem in seismic inversion with conventional TV regularization. A large regularization parameter may lead to an oversmoothed inversion result, while a small value leads to a noisy inversion result. Another advantage of HTV regularization is that it can generate proper inversion results even if a regularization parameter that is too large is adopted, which makes it easy to set the value of the regularization parameter. Numerical examples demonstrate the performance of the HTV regularization method proposed in this research.


INDEX TERMS Seismic inversion, seafloor sediment properties, total-variation regularization, sharp boundaries, staircase effect.

I. INTRODUCTION

In exploratory geophysics, seismic inversion is an effective tool used to recover the properties of subsurface strata from the observed wavefield. Due to the inherent ill-posedness of the inversion problem, estimating the subsurface properties with seismograms is a challenging problem [1]. Information on the inverted subsurface properties is easily polluted by inversion errors due to random noise in the observed data. A common approach to mitigate the ill-posedness of the problem is to apply regularization to the inversion process [2]–[5]. In this research, we focus on estimating seafloor elastic parameters with prestack seismic data. It is of vital importance for geological

interpretation to recover high-fidelity inversion results with clear boundaries and textures from noisy prestack seismic data. A hybrid total-variation (HTV) regularization operator is proposed to address the ill-posedness of prestack seismic inversion.

HTV regularization improves conventional total-variation (TV) regularization and shows better performance in seafloor prestack seismic inversion. Conventional total-variation (TV) regularization was first proposed by Rudin *et al.* [6] for image denoising. Owing to its desirable edge-preserving property, TV regularization is widely adopted in various applications, such as electrical impedance tomography [7], [8], bioelectric source imaging [9], [10], inverse wave propagation [11], seismic inversion [12]–[16] and many other fields [17]–[23]. However, TV regularization usually suffers from the staircase effect [24]–[26], which leads to misinterpretations of the

The associate editor coordinating the review of this manuscript and approving it for publication was Geng-Ming Jiang .

strata features. Rather than minimizing the total variation of the elastic parameters as in TV regularization, HTV regularization minimizes the total variation of the zero-mean oscillation component (ZMOC) of the elastic parameters. The ZMOC is obtained by subtracting the local mean of the upper and lower envelopes from the elastic parameters. HTV regularization retains the advantage of TV regularization in edge-preserving properties while effectively eliminating the staircase effect of TV regularization. Therefore, HTV regularization can recover geological boundaries and introduce no staircase artifacts when applied in seafloor prestack seismic inversion. In addition, a proper regularization parameter is of vital importance for the inversion process with conventional TV regularization. Many methods, such as generalized cross-validation [27], [28], the Morozov discrepancy principle [29], the L curve criterion [30] and the Arcangeli criterion [31], have been developed to provide theoretical justification for the appropriate parameter selection. If the regularization parameter is too small, the regularization will not improve the inversion result. If the regularization parameter is too large, the inverse problem can be solved stably, but the result will be too smooth to reveal the geological boundaries and textures. Unlike conventional regularization methods, HTV can generate a proper inversion result even if the regularization parameter is very large. This property makes it easy to choose the regularization parameter when HTV is adopted.

The remainder of this paper is organized as follows: First, we review the background of seafloor prestack inversion and regularization, followed by presentation of the HTV operator. Second, numerical examples are used to study the performance of the HTV regularization operator. Third, a discussion is given to provide deeper insight into the research. Finally, we present conclusions based on the research in this paper.

II. THEORY

A. BACKGROUND

In marine seismic exploration, a source and streamer are towed by the survey vessel. The seismic wave is generated by the source, propagated by seawater, reflected by seabed sediments, and finally received by the streamer (Fig. 1). The seismic wave reflected from the seabed sediment carries information on the sediment properties. Therefore, the observed data from the streamer can be used to invert for seabed sediment properties such as P-wave velocity, S-wave velocity and density.

The relationship between the incidence angle and reflection coefficient at the seafloor is determined by the elastic parameters of seawater and seabed sediment [32], [33]. For seafloor prestack seismic inversion, elastic parameters of seawater, including P-wave velocity and density, are typically treated as known parameters. Therefore, the reflection coefficients for one common reflection point (CRP) at different incidence angles can be determined when the elastic

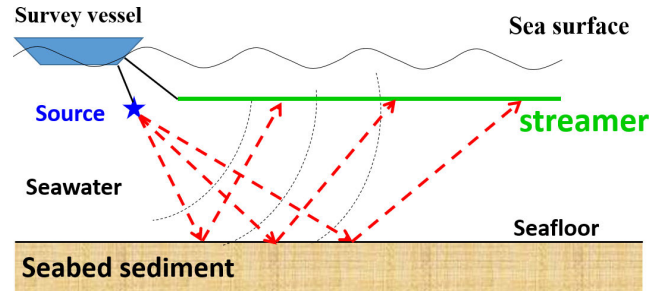


FIGURE 1. Cartoon for marine seismic observation system.

parameters of seabed sediment are given:

$$\mathbf{d} = f(\mathbf{m}) \quad (1)$$

where $\mathbf{d} = [d_1 \ d_2 \ \dots \ d_k]$ is the reflection coefficients for one CRP at a given incidence angle $\theta = [\theta_1 \ \theta_2 \ \dots \ \theta_k]$. $\mathbf{m} = [\alpha \ \beta \ \rho]$ denotes the elastic parameters of the seabed sediment at the reflection point with each component α , β and ρ denoting P-wave velocity, S-wave velocity and density, respectively.

The data acquisition process of a two-dimensional seismic survey can be mathematically formulated as

$$\mathbf{D} = A(\mathbf{M}) + \mathbf{n} \quad (2)$$

where $\mathbf{D} = [\mathbf{d}_1 \ \mathbf{d}_2 \ \dots \ \mathbf{d}_n]^T$ denotes the observed data for all CRPs along the seismic survey, which are further used to invert for the model parameter $\mathbf{M} = [\mathbf{m}_1 \ \mathbf{m}_2 \ \dots \ \mathbf{m}_n]$. The vector \mathbf{n} is additive random noise generated in the acquisition process. The functional A stands for a forward modeling operator that differs for different problems.

The inversion process to estimate the model parameter \mathbf{M} with the observed data \mathbf{D}^{obs} is commonly achieved by least-square data fitting.

$$\arg \min_{\mathbf{M}} \|A(\mathbf{M}) - \mathbf{D}^{obs}\|^2 \quad (3)$$

The above inversion problem is typically ill-posed, and the inversion results are not stable. A common way to surmount this problem is to use regularization methods, in which a regularization term is introduced to restrict the solutions:

$$\arg \min_{\mathbf{M}} \|A(\mathbf{M}) - \mathbf{D}^{obs}\|^2 + \lambda R(\mathbf{M}) \quad (4)$$

where λ is a positive regularization parameter that plays an important role in balancing the trade-off between the regularization process and the data-fitting process. Total variation regularization was first proposed by Rudin *et al.* [6], and is widely used in different kinds of problems. For the seafloor prestack inversion problem, the TV regularization function $R(\mathbf{M})$ can be written as

$$R(\mathbf{M}) = \sum_{i=1}^{n-1} |\mathbf{m}_i - \mathbf{m}_{i+1}| \quad (5)$$

Equation (5) corresponds to the spatial gradient of the model parameter \mathbf{M} , and minimizing (4) will effectively attenuate the high gradient parts such as the inversion errors

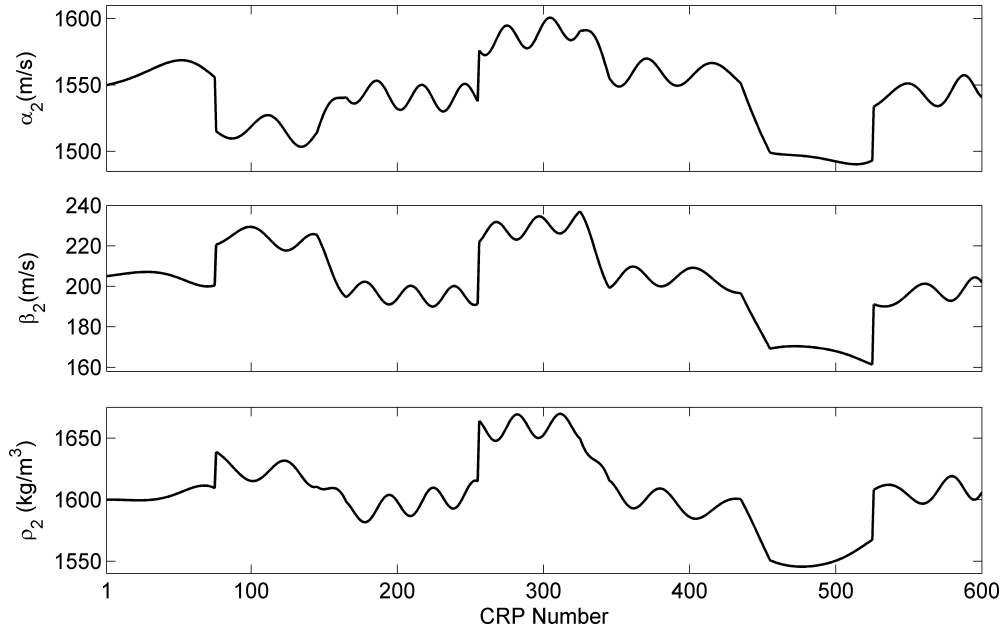


FIGURE 2. Elastic parameter model for the seafloor sediments. The horizontal axis denotes different locations for different CRP numbers. The vertical axes are the P-wave velocity, S-wave velocity and density of the seafloor sediments.

due to the noisy data. The essence of TV regularization is to transform the oscillation inversion result into a piecewise-constant result, which is also called the staircase effect. The staircase effect leads to strong artifacts in the inversion result. One other disadvantage of the TV approach is its tendency to uniformly penalize the image gradient irrespective of the underlying image structures. As a result, edges, especially those of low contrast regions, are sometimes oversmoothed, leading to loss of low contrast information. To address these shortcomings, we propose an HTV regularization operator.

B. HTV REGULARIZATION OPERATOR

It is clear that in (4), the real model parameter and the inversion error are regularized simultaneously. Rather than minimizing the total variation of the elastic parameters as in TV regularization, HTV regularization minimizes the inversion error of the elastic parameters. Consider that the inversion result \mathbf{M} from (3) with noisy observed data \mathbf{D}^{obs} is composed of two parts:

$$\mathbf{M} = \mathbf{M}^r + \mathbf{M}^e \tag{6}$$

where \mathbf{M}^r is the real model parameter and \mathbf{M}^e is the inversion error from the random noise in the observed data. Since (5) is a linear function, the regularization term in (4) can be written as:

$$R(\mathbf{M}) = R(\mathbf{M}^r) + R(\mathbf{M}^e) \tag{7}$$

From (7), it is clear that the desirable model parameter \mathbf{M}^r is regularized simultaneously with the inversion error \mathbf{M}^e when (5) is applied. The abovementioned disadvantages of TV regularization can be eliminated when only inversion

error \mathbf{M}^e is regularized. Therefore, the following equation is proposed for seafloor prestack inversion.

$$\arg \min_{\mathbf{M}} \|A(\mathbf{M}) - \mathbf{D}^{obs}\|^2 + \lambda R(\mathbf{M}^e) \tag{8}$$

However, the inversion error \mathbf{M}^e is unknown. Therefore, it is impossible to formulate the regularization in (8) directly. In this research, we propose to use the ZMOC to approximate \mathbf{M}^e . The ZMOC is obtained by subtracting the local mean of the upper and lower envelopes from the elastic parameters in the inversion process.

$$\mathbf{M}^e \approx \mathbf{M} - \varphi(\mathbf{M}) \tag{9}$$

where the functional $\varphi(\cdot)$ gives the average of the upper and lower envelopes of its input, which is used to approximate \mathbf{M}^r . Therefore, (8) can be written as

$$\arg \min_{\mathbf{M}} \|A(\mathbf{M}) - \mathbf{D}^{obs}\|^2 + \lambda R(\mathbf{M} - \varphi(\mathbf{M})) \tag{10}$$

There is no analytical solution for (10), gradient-based optimization methods can be used to solve it. When solving (10) with a gradient-based optimization method, the inversion result without regularization from (3) can be adopted as the initial model. To help readers understand the inversion process with HTV regularization method, a brief algorithm (Algorithm 1) is given as follows:

As presented by Algorithm 1, the inversion without regularization is first performed to generate nonregularized inversion result \mathbf{M}^{non} . The comprehensive and detailed methods for the inversion without regularization can be found in the previous researches [32], [34]–[36]. Then, the nonregularized inversion result \mathbf{M}^{non} is adopted as an initial model for the HTV regularization inversion. With \mathbf{M}^{non}

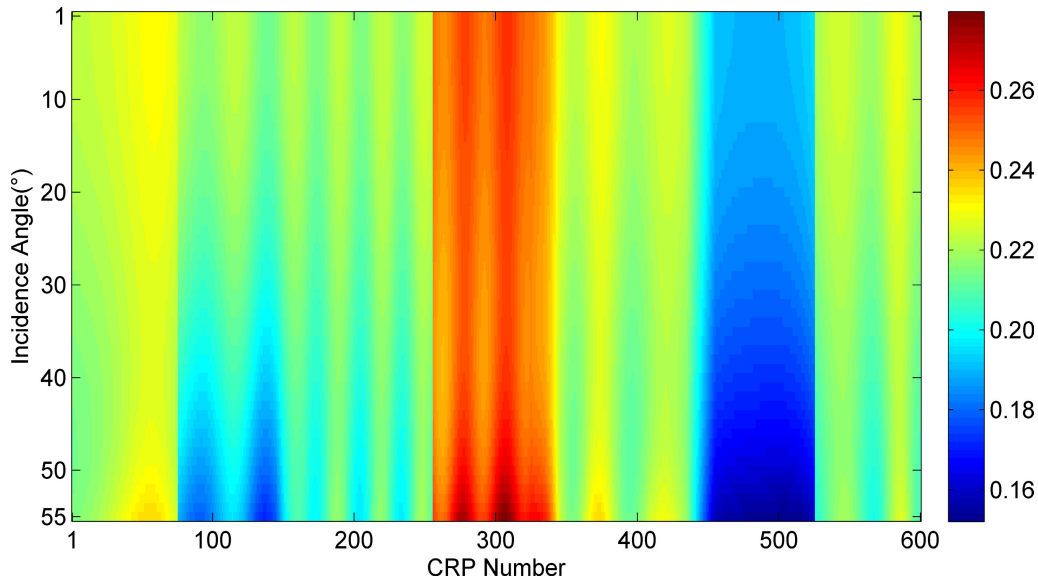


FIGURE 3. Reflection coefficient for the model parameters. The vertical axis is the incidence angle, while the horizontal axis denotes the CRP number. The color bar gives the value of the reflection coefficient.

Algorithm 1 Implementation of the Proposed HTV Regularization Method

Input:

·Observed data \mathbf{D}^{obs} from the seismic survey with n CRPs, $\mathbf{D} = [\mathbf{d}_1 \ \mathbf{d}_2 \ \dots \ \mathbf{d}_n]^T$.

Inversion without regularization:

·Solve (3) under \mathbf{D}^{obs} and then obtain the nonregularized inversion result \mathbf{M}^{non} for the n CRPs, $\mathbf{M}^{non} = [\mathbf{m}_1^{non} \ \mathbf{m}_2^{non} \ \dots \ \mathbf{m}_n^{non}]$.

HTV regularization inversion:

·Set \mathbf{M}^{non} as initial model;

·Solve (10) and obtain the final inversion result \mathbf{M} for the n CRPs of the seismic survey, $\mathbf{M} = [\mathbf{m}_1 \ \mathbf{m}_2 \ \dots \ \mathbf{m}_n]$.

Output:

·The final inversion result \mathbf{M} .

as the initial model, equation (10) can be solved by the gradient-based method [34], [35].

III. NUMERICAL EXAMPLES

Numerical examples are used to investigate the performance of the HTV regularization method in this section. A two-dimensional seismic survey with seafloor elastic property distribution illustrated in Fig. 2, is adopted to demonstrate the advantages of the HTV regularization.

The elastic properties of seawater are typically set as known parameters with a P-wave velocity of 1530 m/s and density of 1030 kg/m³. The reflection coefficient data for all the CRPs are computed for 55 equally spaced incidence angles from 1° to 55° (Fig. 3).

Independent, zero-mean Gaussian random error noise levels of 0.25%, 0.5% and 0.75% are added to the noise-free reflection coefficient to produce the observed data.

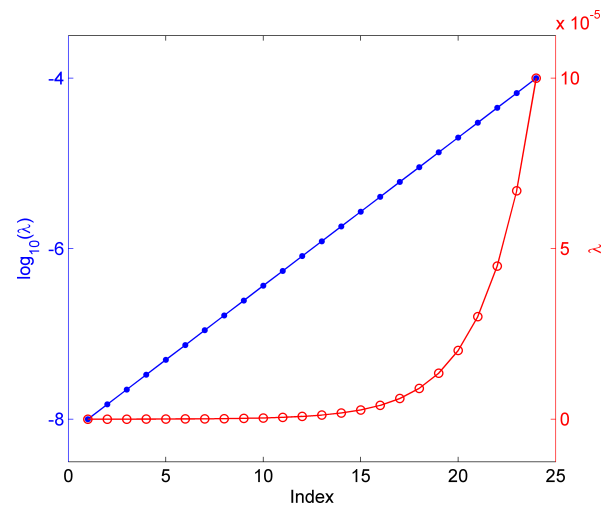


FIGURE 4. Regularization parameter used for inversion. The red dots give the values of the regularization parameters λ (right vertical axis). The blue dots give the values of λ measured in logarithm base-10 (left vertical axis).

The noise level of the random errors is defined as (10) in Liu and Liu [35]. The inversion process is performed for different regularization parameter settings (24 logarithm base-10 values equally spaced in the range of -8 to -4) with results shown in Fig. 4. The regularization parameter plays a balancing role between data fitting and regularization. Fig. 5 gives the relationship between data fitting and regularization when regularization parameters in Fig. 4 are adopted under different noise levels.

In Fig. 5, the “Misfit” axis denotes the value of the data misfit term $\|A(\mathbf{M}) - \mathbf{D}^{obs}\|^2$ of the objective function (4), and the “RG” axis stands for the value of the regularization function (5) $R(\mathbf{M})$, where \mathbf{M} is the inversion result under

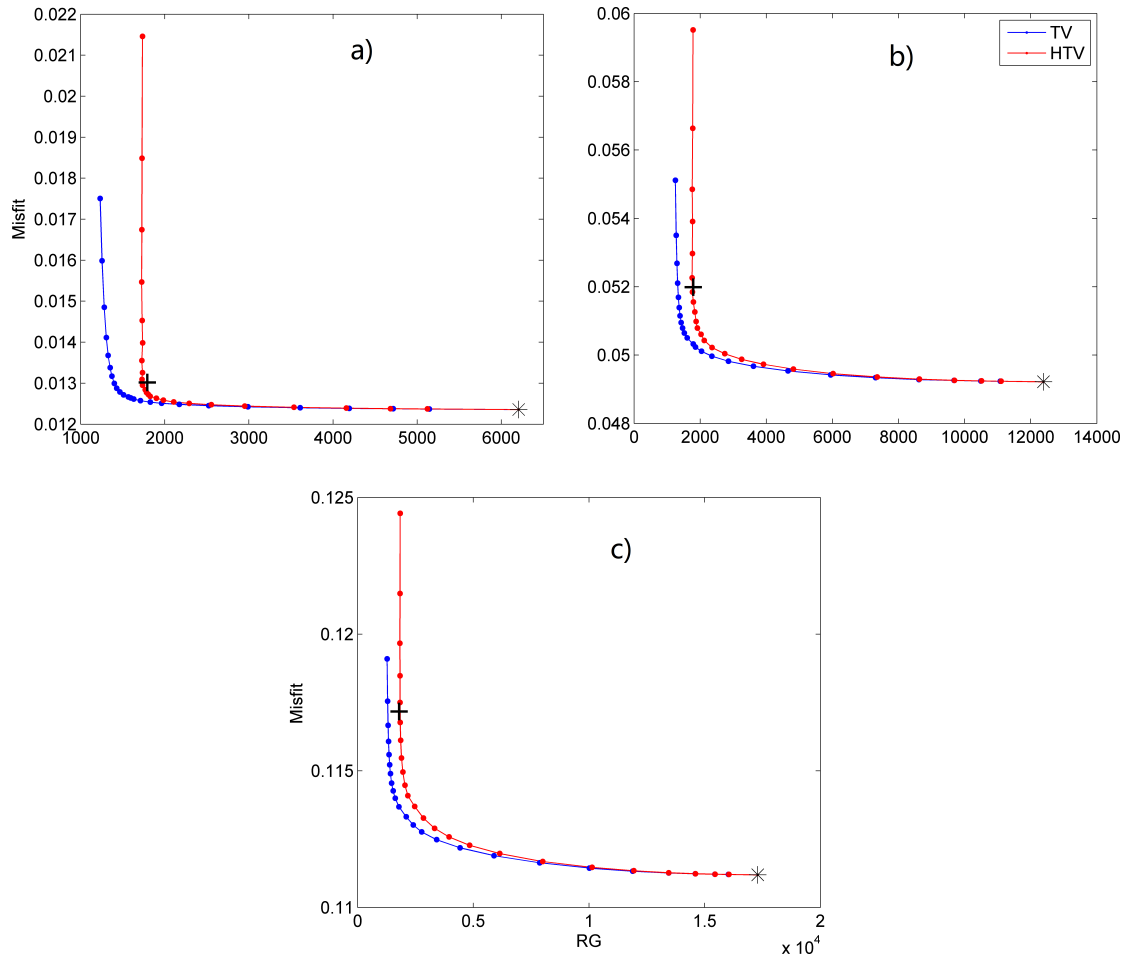


FIGURE 5. The “L” curves for different noise levels. Panels a), b) and c) are from the inversion process with observed data with noise levels at 0.25%, 0.5% and 0.75%, respectively.

a certain regularization parameter. The symbols “+” are obtained with the model parameters given by Fig. 2, while the symbols “*” are calculated with the inversion result without regularization. The red curves are obtained with the inversion result from the method proposed in this research. The blue curves are calculated with the inversion result from the conventional TV regularization method. All the curves are L-shaped and are usually named the “L curve”. With the increase in regularization parameters, the RG decreases and the misfit increases. As the RG decreases, the difference between the red and blue curves becomes increasingly obvious. When RG decreases to the value around “+”, the RG of the red curves stops decreasing, while that of the blue curves continues decreasing. This means that the TV will generate oversmoothed inversion results if the regularization parameter is too large. However, the HTV will not generate oversmoothed inversion results even if the regularization parameter is too large. As a general rule, the proper regularization parameter for TV regularization is selected from the corner of the L curve where the curvature is the maximum [30]. However, the maximum curvature point is not easily determined.

Fig. 6 further illustrates the least-square misfit between the inversion results from the regularization methods and inversion results without regularization.

The horizontal axis is the value of the regularization measured in logarithm base-10, while the vertical axis (Misfit-nonREG) is the misfit between the nonregularization inversion result and the regularized inversion result $||\mathbf{M}^{non} - \mathbf{M}||^2$. The red and blue curves are calculated with the results from the HTV regularization and the conventional TV regularization methods, respectively. It is clear that the Misfit-nonREG grows as the regularization parameter increases. Both TV and HTV curves can be divided into two parts by their points at approximately $\lambda = 10^{-6}$. The Misfit-nonREG grows rapidly as the regularization parameter increases from 10^{-8} to 10^{-6} . When the regularization parameter increases from 10^{-6} to 10^{-4} , the Misfit-nonREG grows slowly. In particular, the growth rate of the HTV curves is similar to that of the TV curves when the regularization parameter is lower than 10^{-6} , while the growth rate of the HTV curves becomes lower than that of the TV curves when the regularization parameter is larger than 10^{-6} . As the regularization parameter increases

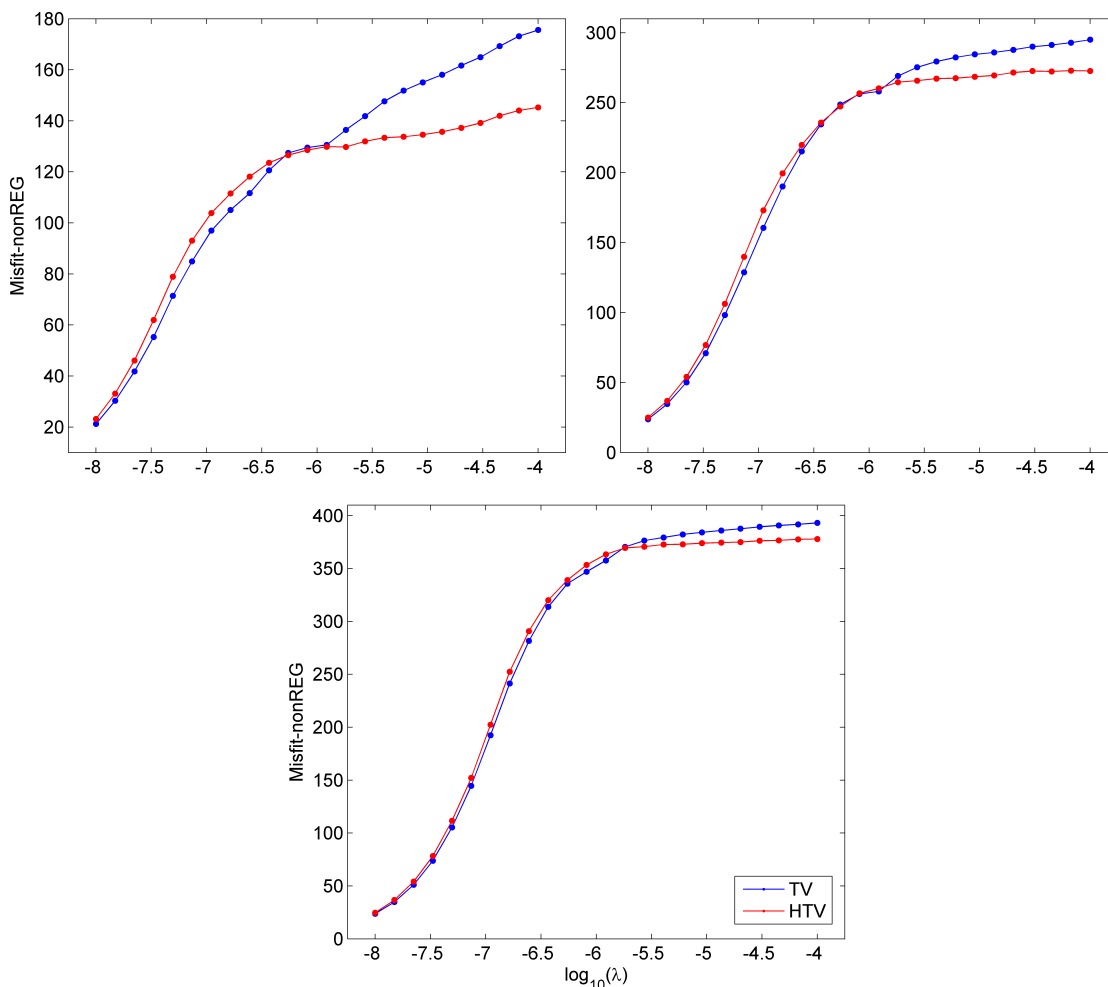


FIGURE 6. Misfit between regularized inversion and nonregularized inversion. Panels a), b) and c) are from the inversion process with observed data with noise levels at 0.25%, 0.5% and 0.75%, respectively.

to 10^{-6} , the inversion error caused by the random noise in the observed data is attenuated and gradually suppressed. Conventional TV regularization generates an oversmoothed result when the regularization parameter is larger than 10^{-6} , which leads to the continued growth of the Misfit-nonREG. The HTV regularization method does not continue smoothing the inversion result as the regularization parameter increases larger than 10^{-6} . Therefore, the growth of Misfit-nonREG suddenly slows down when the regularization parameter reaches 10^{-6} . Fig. 7 gives a comparison of the inversion results from different inversion methods.

The inversion result without regularization is polluted by oscillating inversion errors. As studied by Liu and Liu [35], the S-wave velocity is the most susceptible to random noise in the observed data, while the P-wave velocity and density are susceptible to a lesser extent. It is clear that the oscillating artifacts are effectively suppressed when regularization is adopted. While both the TV and HTV regularization methods generate similar results for P-wave velocity and density, they generate different inversion results for S-wave velocity. The inversion result from TV for S-wave velocity is combined

with piecewise constant values like a staircase along the inversion result without regularization. However, the result from HTV for S-wave velocity is much smoother without the staircase effect when fitting the inversion result without regularization. Fig. 8 gives more detailed information of Fig. 7 by local magnification from CRP numbers 255 to 350.

Although the results from TV and HTV show slight differences in P-wave velocity and density, they are both acceptable for the following interpretation process. However, the obvious staircase artifacts in the TV result for S-wave velocity make the result a poor candidate for interpretation. The result from the HTV regularization method properly describes the elastic distribution of the seafloor sediments. It is not always easy to determine the proper regularization parameter for regularization inversion. A small regularization parameter leads to a noisy inversion result. A large regularization parameter may lead to an oversmoothed inversion result for conventional TV regularization, while the HTV regularization method gives acceptable results under a large regularization parameter. Fig. 9 illustrates the inversion results under regularization parameters 10^{-4} .

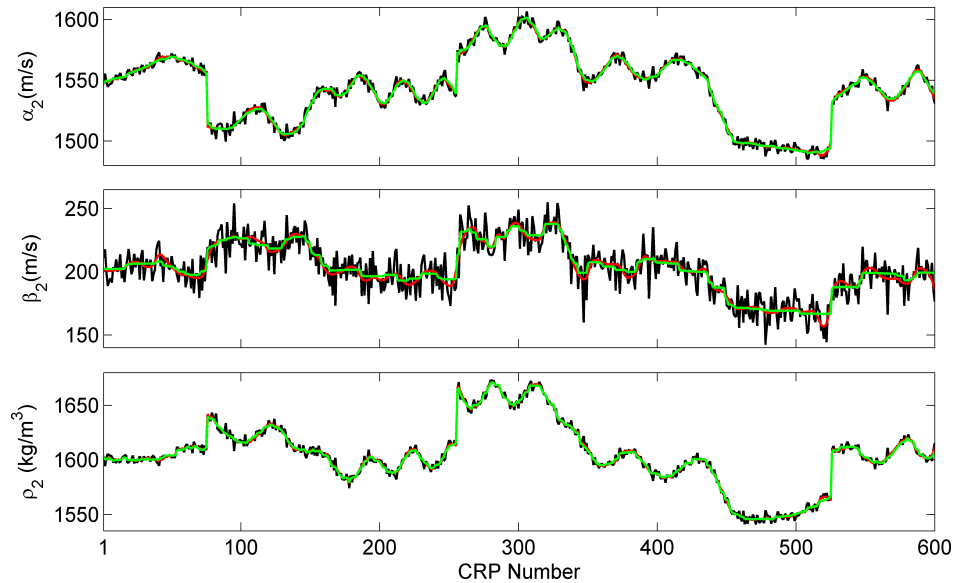


FIGURE 7. Inversion result when $\lambda = 10^{-6}$. The three panels from top to bottom are the inversion results for P-wave velocity, S-wave velocity and density. The black curves denote the inversion result without regularization, while the green and red curves are the inversion results from conventional TV regularization and the method proposed in this research, respectively.

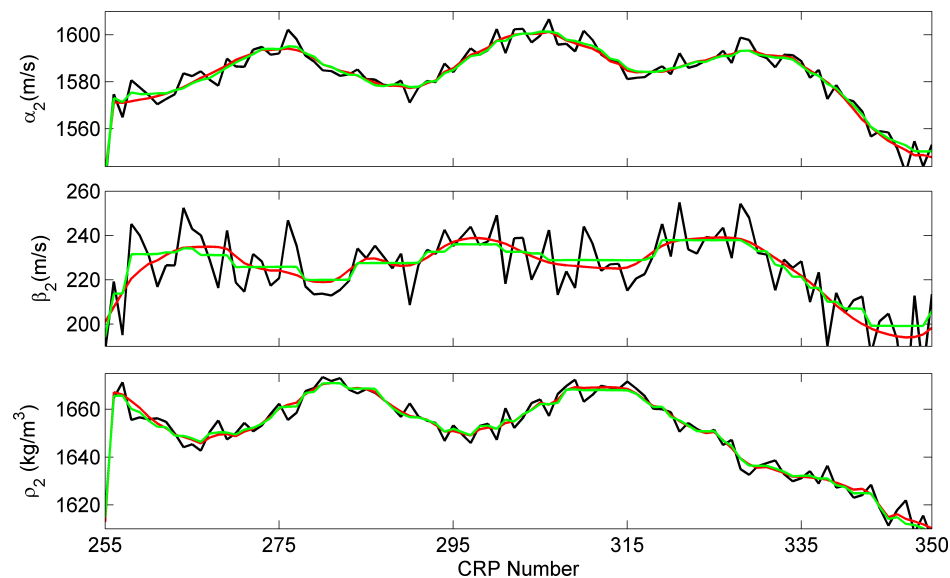


FIGURE 8. Local zoomed inversion result when $\lambda = 10^{-6}$. The curves have the same meaning as those in Fig. 7.

It is clear that the S-wave velocity from the TV regularization method is obviously oversmoothed by piecewise constant stairs, while that from the HTV method can properly give the S-wave velocity distribution. The oversmoothed result from TV will lead to misinterpretations that have lost textures of the sediment distribution. In fact, the P-wave velocity and density from TV are also oversmoothed by piecewise constant stairs. Fig. 10 illustrates the details of the inversion result by local magnification of Fig. 9 from CRP numbers 255 to 350. From Fig. 10, we can see that the staircase effect of density is much more obvious than that of P-velocity for the TV regularization method. All three

parameters from HTV can still properly describe the sediment distribution.

IV. DISCUSSION

TV regularization can preserve the sharp boundaries while effectively suppressing inversion errors. The regularization parameter plays an important role in balancing the trade-off between the regularization term and the data-misfit term. The optimal choice of regularization parameters should take these two cases into account. Too small a regularization parameter may produce underregularized inversion results. Conversely, too much regularization may be imposed on the inversion

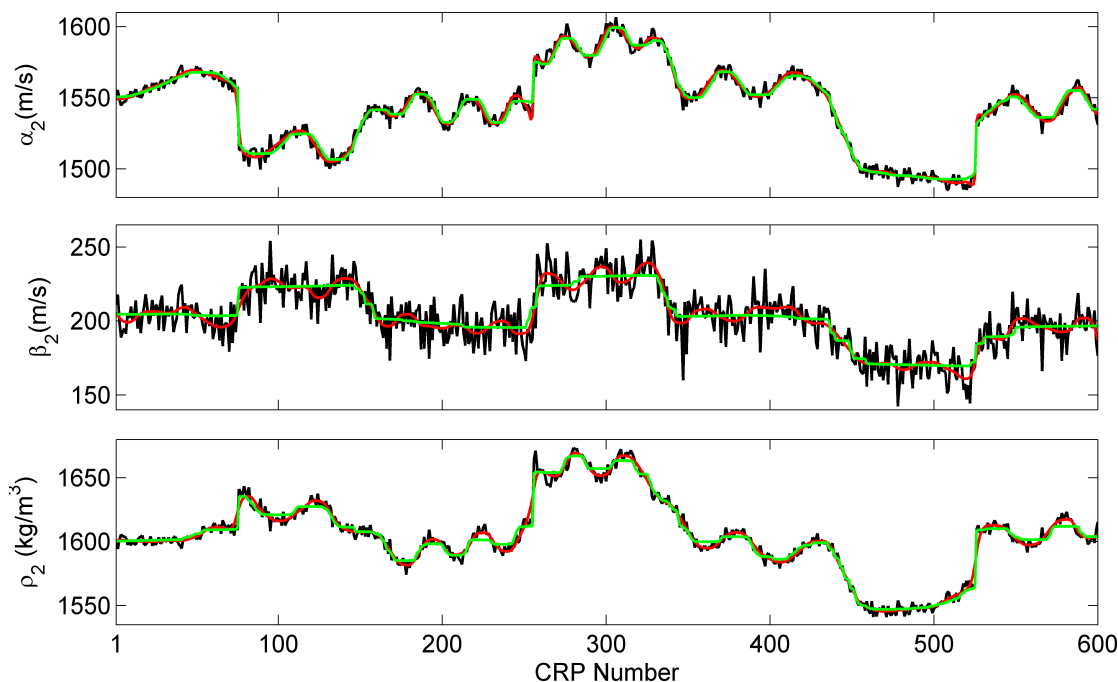


FIGURE 9. Inversion result when $\lambda = 10^{-4}$. The curves have the same meaning as those in Fig. 7.

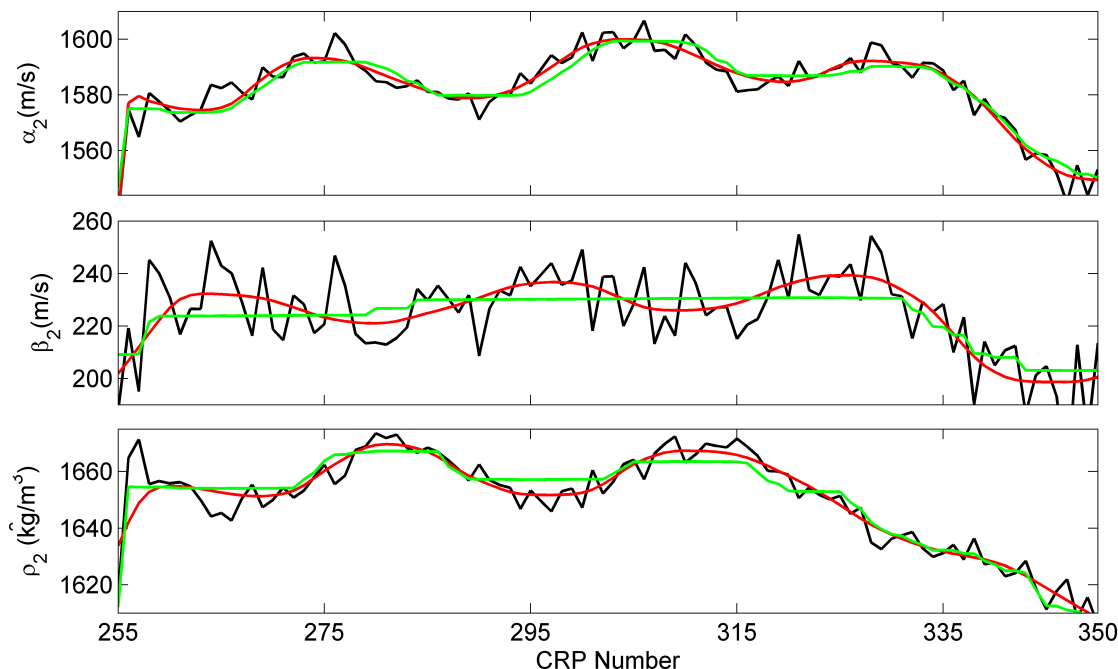


FIGURE 10. Local zoomed inversion result when $\lambda = 10^{-4}$. The curves have the same meaning as those in Fig. 7.

if the regularization parameter is too large. The underregularized inversion result suffers from inversion errors, which makes it difficult to interpret the geological features of the subsurface strata. Although the overregularized inversion result is stable and clean from the oscillation errors, it does not present the distribution of the sediments properly, which is also not acceptable for the interpretation process. Since HTV regularization only minimizes the ZMOC of the elastic

parameters, it does not produce an overregularized inversion result even if the regularization parameter is too large. This property makes it easy to determine the regularization parameter when HTV regularization is adopted.

Another drawback of conventional TV regularization applied in seismic prestack inversion is its staircase effect. The staircase effect is most obvious for S-wave velocity, less so for density and the least for P-wave velocity. Although the

inversion errors can be suppressed, the staircase effect brings artifacts to the interpretation process. HTV regularization has no staircase effect and can generate proper inversion results to illustrate the distribution of seafloor sediments.

V. CONCLUSION

It is important to recover high-fidelity elastic parameters of seafloor sediments from noisy prestack seismic data. Conventional TV regularization can suppress inversion errors and preserve the sharp boundaries of the subsurface strata. However, it always suffers from the staircase effect, and the regularization parameter is not easily determined. A hybrid regularization operator is proposed and applied in prestack seismic inversion. HTV regularization does not oversmooth the inversion result under a large regularization parameter, so the regularization parameter is easy to determine. The HTV has good edge-preservation performance but does not suffer from the staircase effect. Numerical examples prove the performance of the HTV regularization method proposed in this research.

ACKNOWLEDGMENT

Thanks to the editor and reviewers for their valuable comments that helped to improve the manuscript.

REFERENCES

- [1] A. Tarantola, *Inverse Problem Theory and Methods for Model Parameter Estimation*. Philadelphia, PA, USA: Society for Industrial & Applied Mathematics, 2005.
- [2] H. W. Engl, M. Hanke, and A. Neubauer, *Regularization of Inverse Problems*. Amsterdam, The Netherlands: Springer, 2000.
- [3] D. L. Phillips, "A technique for the numerical solution of certain integral equations of the first kind," *J. Assoc. Comput. Mach.*, vol. 9, no. 1, pp. 84–97, Jan. 1962, doi: [10.1145/321105.321114](https://doi.org/10.1145/321105.321114).
- [4] A. N. Tikhonov, "Regularization of incorrectly posed problems," *Doklady Akademii Nauk SSSR*, vol. 153, no. 1, p. 49, 1963.
- [5] Y. Wang, *Seismic Inversion: Theory and Applications*. U.K.: Wiley, 2016.
- [6] L. I. Rudin, S. Osher, and E. Fatemi, "Nonlinear total variation based noise removal algorithms," *Phys. D, Nonlinear Phenomena*, vol. 60, nos. 1–4, pp. 259–268, 1992.
- [7] A. Borsic, B. M. Graham, A. Adler, and W. Lionheart, "In vivo impedance imaging with total variation regularization," *IEEE Trans. Med. Imag.*, vol. 29, no. 1, pp. 44–54, Jan. 2010, doi: [10.1109/TMI.2009.2022540](https://doi.org/10.1109/TMI.2009.2022540).
- [8] E. T. Chung, T. F. Chan, and X.-C. Tai, "Electrical impedance tomography using level set representation and total variational regularization," *J. Comput. Phys.*, vol. 205, no. 1, pp. 357–372, May 2005, doi: [10.1016/j.jcp.2004.11.022](https://doi.org/10.1016/j.jcp.2004.11.022).
- [9] L. Ding and B. He, "Sparse source imaging in electroencephalography with accurate field modeling," *Hum. Brain Mapping*, vol. 29, no. 9, pp. 1053–1067, 2010.
- [10] S. Ghosh and Y. Rudy, "Application of L1-norm regularization to epicardial potential solution of the inverse electrocardiography problem," *Ann. Biomed. Eng.*, vol. 37, no. 5, pp. 902–912, Mar. 2009, doi: [10.1007/s10439-009-9665-6](https://doi.org/10.1007/s10439-009-9665-6).
- [11] V. Akcelik, G. Biros, and O. Ghattas, "Parallel multiscale Gauss-Newton-Krylov methods for inverse wave propagation," in *Proc. ACM/IEEE Conf. Supercomput. (SC)*, Baltimore, MD, USA, Nov. 2002, p. 41.
- [12] A. Guitton, "Blocky regularization schemes for full-waveform inversion," *Geophys. Prospecting*, vol. 60, no. 5, pp. 870–884, Sep. 2012, doi: [10.1111/j.1365-2478.2012.01025.x](https://doi.org/10.1111/j.1365-2478.2012.01025.x).
- [13] Y. Lin and L. Huang, "Acoustic- and elastic-waveform inversion using a modified total-variation regularization scheme," *Geophys. J. Int.*, vol. 200, no. 1, pp. 489–502, Jan. 2014, doi: [10.1093/gji/ggu393](https://doi.org/10.1093/gji/ggu393).
- [14] Y. Liu, Y. Zhong, K. Liu, and Q. Hua, "Seafloor elastic-parameter estimation based on a regularized AVO inversion method," *Mar. Geophys. Res.*, vol. 41, no. 1, Feb. 2020, doi: [10.1007/s11001-020-09405-x](https://doi.org/10.1007/s11001-020-09405-x).
- [15] E. TikEsser, L. Guasch, T. van Leeuwen, A. Y. Aravkin, and F. J. Herrmann, "Total variation regularization strategies in full-waveform inversion," *SIAM J. Imag. Sci.*, vol. 11, no. 1, pp. 376–406, Feb. 2018, doi: [10.1137/17m111328x](https://doi.org/10.1137/17m111328x).
- [16] P. Yong, W. Y. Liao, J. Huang, and Z. Li, "Total variation regularization for seismic waveform inversion using an adaptive primal dual hybrid gradient method," *Inverse Problems*, vol. 34, no. 4, p. 23, Apr. 2018, doi: [10.1088/1361-6420/aaaf8e](https://doi.org/10.1088/1361-6420/aaaf8e).
- [17] J.-J. Wang, T.-Z. Huang, J. Huang, and L.-J. Deng, "A two-step iterative algorithm for sparse hyperspectral unmixing via total variation," *Appl. Math. Comput.*, vol. 401, Jul. 2021, Art. no. 126059, doi: [10.1016/j.amc.2021.126059](https://doi.org/10.1016/j.amc.2021.126059).
- [18] D. Qiu, M. Bai, M. K. Ng, and X. Zhang, "Robust low-rank tensor completion via transformed tensor nuclear norm with total variation regularization," *Neurocomputing*, vol. 435, pp. 197–215, May 2021, doi: [10.1016/j.neucom.2020.12.110](https://doi.org/10.1016/j.neucom.2020.12.110).
- [19] J. Guo and Q. Chen, "Image denoising based on nonconvex anisotropic total-variation regularization," *Signal Process.*, vol. 186, Sep. 2021, Art. no. 108124, doi: [10.1016/j.sigpro.2021.108124](https://doi.org/10.1016/j.sigpro.2021.108124).
- [20] W. Lu, J. Duan, Z. Qiu, Z. Pan, R. W. Liu, and L. Bai, "Implementation of high-order variational models made easy for image processing," *Math. Methods Appl. Sci.*, vol. 39, no. 14, pp. 4208–4233, 2016, doi: [10.1002/mma.3858](https://doi.org/10.1002/mma.3858).
- [21] Q. Shu, C. Wu, Q. Zhong, and R. W. Liu, "Alternating minimization algorithm for hybrid regularized variational image dehazing," *Optik*, vol. 185, pp. 943–956, May 2019, doi: [10.1016/j.ijleo.2019.04.002](https://doi.org/10.1016/j.ijleo.2019.04.002).
- [22] R. W. Liu, L. Shi, W. Huang, J. Xu, S. C. Yu, and D. Wang, "Generalized total variation-based MRI Rician denoising model with spatially adaptive regularization parameters," *Magn. Reson. Imag.*, vol. 32, no. 6, pp. 702–720, Jul. 2014, doi: [10.1016/j.mri.2014.03.004](https://doi.org/10.1016/j.mri.2014.03.004).
- [23] J. Tang, "Nonconvex and nonsmooth total variation regularization method for diffuse optical tomography based on RTE," *Inverse Problems*, vol. 37, no. 6, Apr. 2021, Art. no. 065001, doi: [10.1088/1361-6420/abf5ed](https://doi.org/10.1088/1361-6420/abf5ed).
- [24] M. Benning, C. Brune, M. Burger, and J. Müller, "Higher-order TV methods—Enhancement via Bregman iteration," *J. Sci. Comput.*, vol. 54, nos. 2–3, pp. 269–310, Feb. 2013, doi: [10.1007/s10915-012-9650-3](https://doi.org/10.1007/s10915-012-9650-3).
- [25] T. Chan, A. Marquina, and P. Mulet, "High-order total variation-based image restoration," *SIAM J. Sci. Comput.*, vol. 22, no. 2, pp. 503–516, Aug. 2000, doi: [10.1137/s1064827598344169](https://doi.org/10.1137/s1064827598344169).
- [26] M. Ding, T.-Z. Huang, S. Wang, J.-J. Mei, and X.-L. Zhao, "Total variation with overlapping group sparsity for deblurring images under Cauchy noise," *Appl. Math. Comput.*, vol. 341, pp. 128–147, Jan. 2019, doi: [10.1016/j.amc.2018.08.014](https://doi.org/10.1016/j.amc.2018.08.014).
- [27] P. Craven and G. Wahba, "Smoothing noisy data with spline functions: Estimating the correct degree of smoothing by the method of generalized cross-validation," *Numerische Math.*, vol. 31, no. 4, pp. 377–403, Dec. 1978.
- [28] G. H. Golub, M. Heath, and G. Wahba, "Generalized cross-validation as a method for choosing a good ridge parameter," *Technometrics*, vol. 21, no. 2, pp. 215–223, May 1979, doi: [10.2307/1268518](https://doi.org/10.2307/1268518).
- [29] V. A. Morozov, *On Regularization of Ill-Posed Problems and Selection of Regularization Parameter*. New York, NY, USA: Springer, 1984.
- [30] P. C. Hansen, "Analysis of discrete ill-posed problems by means of the L-curve," *SIAM Rev.*, vol. 34, no. 4, pp. 561–580, Dec. 1992, doi: [10.1137/1034115](https://doi.org/10.1137/1034115).
- [31] C. W. Groetsch, *The Theory of Tikhonov Regularization for Fredholm Equations of the First Kind*. New York, NY, USA: Pitman, 1984.
- [32] Y. Liu, U. Tinivella, and X. Liu, "An inversion method for seafloor elastic parameters," *Geophysics*, vol. 80, no. 3, pp. N11–N21, May 2015, doi: [10.1190/geo2014-0028.1](https://doi.org/10.1190/geo2014-0028.1).
- [33] M. Riedel and F. Theilen, "AVO investigations of shallow Marine sediments," *Geophys. Prospecting*, vol. 49, no. 2, pp. 198–212, Mar. 2001, doi: [10.1046/j.1365-2478.2001.00246.x](https://doi.org/10.1046/j.1365-2478.2001.00246.x).
- [34] Y. Liu and X. Liu, "Application and performances of unconstrained optimization methods in seafloor AVO inversion," *Arabian J. Geosci.*, vol. 9, no. 15, Oct. 2016, Art. no. 652.
- [35] Y. Liu and X. Liu, "Seafloor elastic parameters estimation based on AVO inversion," *Mar. Geophys. Res.*, vol. 36, no. 4, pp. 335–342, Dec. 2015.
- [36] Y. Liu, X. Liu, and H. Ning, "Analysis and improvement for a linearized seafloor elastic parameter inversion method," *J. Appl. Geophys.*, vol. 128, pp. 110–114, May 2016.



YANGTING LIU received the Ph.D. degree in geophysics from China University of Geosciences, Beijing, China, in 2017.

Since 2017, he has been an Assistant Researcher with the First Institute of Oceanography, Ministry of Natural Resources, China, and Qingdao National Laboratory for Marine Science and Technology, Qingdao. His research interests include geophysical information processing and inversion theory.



CHENGLIANG XIE received the master's degree from China University of Geosciences, Beijing, China, in 2013.

Since 2013, he has been affiliated with Guangzhou Marine Geological Survey, Guangzhou, China. His research interests include marine seismic data processing and parallel computing.



CHENGUANG LIU received the master's degree in marine geology from the First Institute of Oceanography, Ministry of Natural Resources, China, in 2003.

He is currently a Senior Engineer with the First Institute of Oceanography, Ministry of Natural Resources, and Qingdao National Laboratory for Marine Science and Technology, Qingdao. He is mainly engaged in marine geophysical investigation and research work.



QING-XIAN ZHAO received the master's degree from Jilin University, Changchun, China, in 2009.

Since 2009, he has been affiliated with Guangzhou Marine Geological Survey, Guangzhou, China. He is currently a Senior Engineer with the rank of professor at Guangzhou Marine Geological Survey. He is mainly engaged in the research and development of marine geophysical equipment and technical methods

...